Environmental Pollution 315 (2022) 120444

Contents lists available at ScienceDirect

Environmental Pollution

journal homepage: www.elsevier.com/locate/envpol

UV stabilizers can foster early development of biofilms on freshwater microplastics☆

Abhrajyoti Tarafdar [a], Ja-yun Lim [b], Jung-Hwan Kwon [a,*]

[a] Division of Environmental Science and Ecological Engineering, Korea University, Seoul, 02841, Republic of Korea
[b] Department of Clinical Laboratory Science, Hyejeon College, 19 Daehak-1gil, Hongsung-eup, Hongsung-gun, Chungnam, 32244, Republic of Korea

ARTICLE INFO

Keywords:
Plastisphere
LDPE
UV-327
UV-531
Toxicity
Oxidative stress
Biofilm

ABSTRACT

Interactions between microbes and microplastics are important as of emerging plastic loads in the global environment. Although diverse plastic additives are used in large amounts, there are very few studies on a quantitative comparison of plastisphere on plastics with different plastic additives. We studied the effects of two widely used UV stabilizers (benzotriazole-type UV-327 and benzophenone-type UV-531 were selected based on their persistence and toxicity) in low-density polyethylene (LDPE) on freshwater microbes. This is the first study on the sole effects of UV stabilizers used as plastic additives on freshwater *in situ* plastisphere biofilm development. Confocal laser scanning microscopy, assisted with proper differentiating fluorochromes and threshold-based 3D segmentation of data, was used to visualize and quantify biofilm. On the first week of biofilm growth, there was very little biovolume and a negligible amount of phototrophs on pristine LDPE contrasting other substrates. Biovolumes were significantly higher on LDPE with UV stabilizers (up to 159% higher than pristine LDPE), although the biomass was mostly dead due to toxicity (>100% higher dead biovolume than live biovolume in LDPE with UV stabilizers). After the fourth week, marginally higher biovolumes along with a revival of the biomass on LDPE with UV stabilizers were observed. The ability to induce microorganismic intracellular reactive oxygen species by UV stabilizers was detected, which may stimulate biofilm growth during the primary phase of biofilm development. Atomic force microscopy analysis denoted that LDPE with UV stabilizers exhibit considerably stronger adhesion force than pristine LDPE. These observations suggest that UV stabilizers can foster the early attachment of microbes to microplastics while killing the surface contacting layer. An alive upper layer of microbes can get developed on the dead biofilm without much disruption due to the toxicity of UV stabilizers. This occurrence can eventually boost the early development of biofilms on plastics.

1. Introduction

The increasing load of plastic particles in the global environment has led the scientific community to study plastic-associated biofilms or 'plastisphere'. Biomass on oceanic plastic waste addresses emerging distress in the delicate oligotrophic marine ecosystems with yet-to-be-known biogeochemical and environmental outcomes (Zhao et al., 2021). Though microplastics in freshwater ecosystems are generally comparable to those found in marine environments, growing evidence often suggests a higher abundance of microplastics in freshwater environments (*i.e.*, lakes and rivers) than that of their oceanic counterparts (de Carvalho et al., 2022; Devereux et al., 2022; Montecinos et al., 2020; Tsering et al., 2022; Xiong et al., 2022). Microplastics generated by various anthropogenic activities are mainly transported to the marine environment via freshwater systems (Huang et al., 2021). Thus, it is necessary to look into microplastic-associated microbial biofilms in freshwater.

Studies on plastisphere characteristics and species abundance of microbes were conducted earlier using commercially available plastics which include various necessary additives (Davidov et al., 2020; De Tender et al., 2017; Di Pippo et al., 2020; Schlundt et al., 2020; Tu et al., 2020; Yang et al., 2021; Zhao et al., 2021). Additive-free pristine

Abbreviations: AFM, atomic force microscopy; CLSM, confocal laser scanning microscopy; CW, Calcofluor white; DAPI, 4,6-diamidino-2-phenylindole; EPS, extracellular polymeric substances; LDPE, low-density polyethylene; ROS, reactive oxygen species.

☆ This paper has been recommended for acceptance by Eddy Y. Zeng.

* Corresponding author.
E-mail addresses: abhra@outlook.com (A. Tarafdar), jayun78@daum.net (J.-y. Lim), junghwankwon@korea.ac.kr (J.-H. Kwon).

https://doi.org/10.1016/j.envpol.2022.120444
Received 7 June 2022; Received in revised form 13 October 2022; Accepted 13 October 2022
Available online 17 October 2022
0269-7491/© 2022 Elsevier Ltd. All rights reserved.

microplastics were also used as substrates to develop and study biofilm characteristics (Gao and Sun, 2021; Miao et al., 2021b; Wright et al., 2021; Ye et al., 2021). Scales et al. (2021) reported that polymer types of different ocean microplastics do not possess any preference in the choice of a microbial community. On the other hand, Cai et al. (2019) observed dissimilarity among bacterial adhesion on different types of commercial plastics with additives. A combination of these studies hints at a hypothesis that different plastic additives may play important parts in shaping the plastisphere. Nonetheless, an extremely modest number of studies have focused on the interactions between microplastics and their likely primary colonizers, highlighting the impacts of specific plastic additives on these microorganisms (Tarafdar et al., 2021). So, there is a huge research gap on the effects of distinct plastic additives on biofilm formation and characteristics, which is vital to illuminate microbial risk as well as a selection of environment-friendly plasticizers (Wang et al., 2022a).

Commercial plastics contain additives including flame retardants, plasticizers, and UV stabilizers, some of which have been shown to affect microbial community composition and functioning (Wright et al., 2020). The sole effect of UV stabilizers on plastisphere development is yet unreported. UV stabilizers are broadly implemented as necessary components in sunscreen-cosmetics merchandise, additives in plastic substances for various outdoor packaging usages, and corrosion inhibitors (Zhang et al., 2011). Amongst them, benzotriazole and benzophenone UV stabilizers are considerably persistent in the ecosystem (Do et al., 2022). Benzotriazole UV stabilizers are suspected to disrupt mitochondrial bioenergetics, embryonic development, locomotor activity in early-stage zebrafish and have immunotoxic effects (Li et al., 2020; Liang et al., 2019, 2017). They were studied to induce oxidative stress on the freshwater green algae *C. reinhardtii* (Giraudo et al., 2017). Benzotriazole UV stabilizers like UV-326, UV-327, and UV-328 were also observed to biomagnify robustly through oceanic food chains (trophic magnification factor, TMF >1) (Wang et al., 2022b). In addition, they may accumulate in the tissues of marine animals and seabirds. For example, UV-327 (2,4-di-*tert*-butyl-6-(5-chlorobenzotriazol-2-yl) phenol) was reported to be one of the most abundant UV stabilizers found in marine debris (Tanaka et al., 2020) and found in the liver of freshwater fish with the highest concentration amongst nine different lipophilic benzotriazole UV stabilizers (65 ng g^{-1} dw) (Wick et al., 2016). UV-327 was enlisted as a substance of very high concern (SVHC) under EU REACH (European Union Registration, Evaluation, and Authorization of Chemicals) due to its great potential for bioaccumulation, persistence in the environment, and toxic effects (ECHA, 2022a). Another widely used benzophenone UV stabilizer, UV-531 ((2-hydroxy-4-(octyloxy)phenyl)(phenyl)methanone) was found to be most abundant in wild freshwater fish with biota–sediment accumulation factor (BSAF) of ~4.88 (Peng et al., 2020). It is recently incorporated into the European Community Rolling Action Plan (CoRAP) for assessment in the forthcoming years (ECHA, 2022b).

From the above literature, we can understand, (1) the importance of studies on freshwater plastisphere, (2) the recent research gap in the effects of distinct plastic additives on plastisphere, and (3) the broad use of UV stabilizers and their possible impact on plastisphere. Consequently, we aimed to observe the sole effects of UV stabilizers on the development of biofilms on the microplastic surface for the first time. The experimentation was designed with the above-mentioned two commonly used UV stabilizers in low-density polyethylene (LDPE) to study their possible toxic effects on the freshwater plastisphere. Especially, to understand the real-life situation, the experiment was conducted *in situ* freshwater streams. This on-site experimental design helped us to deal with the indigenous freshwater plastisphere. Growth of primary biofilms on pristine LDPE, LDPE containing UV stabilizers, and glass were quantified and compared using confocal laser scanning microscopy (CLSM). Oxidative stress in biofilm as a marker of stimulating biofilm growth was observed using the dose-response behavior of fresh biofilms. The adhesion force on plastic surfaces as an indicator of the initial attachment of microbes was also measured using PinPoint™ Nanomechanical mode of atomic force microscopy (AFM) for a mechanistic understanding of biofilm formation and growth.

2. Material and methods

2.1. Materials

Commercial pristine pellets of LDPE (LUTENE® LB5000, density 0.918 g cm^{-3}) were purchased from LG Chem Ltd. (Seoul, Korea). They were cleaned in *n*-hexane for 24 h, dried at room temperature, and stored in an amber glass vial until use.

UV-327 (Product no. 423327, Mol. Wt. 357.88 g mol^{-1}, purity >98%, melting point 150–153 °C) and UV-531 (Product no. 413151, Mol. Wt. 326.43 g mol^{-1}, purity >98%, melting point 47–49 °C) were purchased from Sigma-Aldrich (St. Louis, MO, USA) and their chemical structures are provided in Fig. S1, Supplementary Material. These are among the most commonly used UV stabilizers in LDPE (Hasegawa et al., 2022; Lin et al., 2017). UV absorbers, hindered amine light stabilizers, and quenchers are the three main types of UV stabilizers. Among them, UV absorbers account for over one-fourth of the total global market share (Intelligence, 2021). Benzotriazoles and benzophenones are representative groups of UV absorbers (Markets and Markets, 2022). More than one-third of the total production of UV absorbers is used by the plastic industry (Intelligence, 2021). UV-327 is listed as a substance of very high concern under EU REACH (ECHA, 2022a) and UV-531 is classified as a high production volume chemical (>1000 tons $year^{-1}$) according to OECD (2022).

BacLight Bacterial Viability Kit L13152 and CellROX™ Green Reagent, for cell viability and oxidative stress detection, were purchased from Invitrogen™ (Waltham, MA, USA). DAPI readymade solution (product number MBD0015), Calcofluor white (product number 18909-100 ML-F), and Hoechst 33342 (product number B2261) were procured from Sigma-Aldrich (St. Louis, MO, USA).

2.2. Test-fiber manufacturing and incubations of biofilm

Polyethylene is the most commonly used plastic-type in the plastic industry among all plastics, and it is also the most abundant plastic in marine debris (de Haan et al., 2019; Pabortsava and Lampitt, 2020). LDPE was selected for the study because of its high abundance in the aquatic environment (Liu et al., 2021). Again, the low density allows it to drift in the water, which can increase the availability of the microparticles to the filter feeders (Nalbone et al., 2021).

LDPE fibers (diameter ranging between ~90–160 μm) containing desired mass fraction (1% w/w) of both the UV stabilizers were produced using a Laboratory Mixing Extruder (Dynisco Inc., Franklin, MA, USA). Pristine LDPE pellets were cleaned using *n*-hexane and thereafter put into the hopper (maintained at 170 °C) of the extruder with the desired mass fraction of UV stabilizers. After the first extrusion, the fibers were crushed and put into the extruder two more times to obtain a homogeneous distribution of additives in LDPE. This UV stabilizer mixing process in the pristine LDPE is adopted from Do et al. (2022); which is based on Goff and Whelan (2013). The process is also as per the industrial LDPE manufacturing process by Polychem-USA (2021). Pristine LDPE fibers and glass particles (neutral substrate) were used as controls. Micro-sized (<5 mm) glass particles were selected to grow the freshwater biofilms on an 'inert surface' control matrix (Darrene and Cecile, 2016; van der Kooij et al., 1995).

Two sets of the four samples (i.e., pristine LDPE, LDPE with UV-327, LDPE with UV-531, and glass) were prepared. The fibers and the glass samples were sterilized (70% ethanol), packed in nylon tea bags, and placed 5–6 cm below the surface in a freshwater stream (37°35′10.9″N 127°01′14.8″E, Seongbuk-Cheon, Seoul, South Korea) (Table S1, Supplementary Material). Subsamples were taken at periodic time points (1 and 4 weeks of immersion) and rinsed in phosphate buffer saline to

remove unattached organisms. Samples were dried at room temperature overnight in a Laminar airflow hood and fluorescent dyes were applied immediately before microscopic observations. The scheme of the experimental setup is depicted in Fig. S2, Supplementary Material.

2.3. Fluorophores and staining procedure

Four different fluorophores were used to study the architecture and characteristics of the developed biofilms.

I. SYTO®9 green-fluorescent nucleic acid stain (ex/em: 488/530 nm) for live and propidium iodide (PI) (ex/em: 555/635 nm) for dead microbes (BacLight Bacterial Viability Kit L13152). These stains contrast both in their spectral characteristics and in their ability to infiltrate healthy bacterial cell walls. Microbes with undamaged cell membranes dyed in green were recorded as alive and microbes with broken membranes dyed in red were recorded as non-viable (Hu et al., 2017). The kit was used according to the manufacturer's instructions (Molecular Probes Inc., 2004). Pristine LDPE fibers without biofilm were likewise dyed to bar any misleading positive signs.
II. Photopigments, *Chlorophyll a* (*Chl-a*) (ex/em: 639/660–700 nm) autofluorescence was used for evaluating photosynthetic cells (Miao et al., 2021a), especially diatoms, as they are frequently reported to colonize aquatic plastics (Schlundt et al., 2020).
III. DAPI (4,6-diamidino-2-phenylindole) fluorescent nucleic acid stain (5 μg mL^{-1}, ex/em: 405/470 nm). It is a typical fluorescent dye for the identification and counting of microorganisms like bacteria and protozoa in an aquatic environment. DAPI exhibits an approximately 20-fold improvement of fluorescence upon binding to AT-rich regions of double-stranded DNA minor grooves.
IV. Calcofluor white (CW) (1 g L^{-1} Calcofluor white + 0.05 g L^{-1} Evans blue, ex/em: 380/475 nm) for yeast, fungi, parasitic organism detection; binds to cellulose (α-D-glucopyranose and β-D-glucopyranose polysaccharides) and chitin in cell walls (Sigma-Aldrich, 2021).

For *Chl-a* autofluorescence and biomass visualized by DAPI + CW imaging, all the fiber and glass samples (4 substrates × 2 durations × triplicate = 24 samples) were firstly mounted into a 35 mm glass-bottom confocal dish (SPL Life Sciences Co., Ltd., Pocheon-si, Republic of Korea). Then, 0.25 mL of blue dye solution (0.125 mL of Calcofluor White & Evan's blue solution accompanied with 0.125 mL of DAPI) was applied to the samples and kept in the dark for 15 min at room temperature. Excess dye was thereafter soaked off using paper towels. Samples were washed using phosphate buffer solution and dried in a vacuum desiccator (~30 °C) before CLSM imaging. Biovolumes estimated using the fluorescence of *Chl-a* and DAPI + CW channels are not directly comparable because of the difference in fluorescence intensity between the two channels. However, they can be comparable with the results generated from the same channel.

For Live/Dead imaging, all the fiber and glass samples (4 substrate × 2 durations × triplicate = 24 samples) were incubated with the BacLight fluorescent stains at room temperature (~25 °C) in the dark for 15–20 min and thereafter washed with phosphate buffer solution to remove unbound dyes. After staining, the samples were directly mounted onto 35 mm glass-bottom confocal dishes and subjected to CLSM (Tarafdar et al., 2021). The gain control setup designed for PI was tested to be much lower than the minimum gain control needed for *Chl-a* detection. Live/Dead cell imaging using PI and SYTO-9 has been previously used in numerous studies for algal viability detection (e.g., Cai et al., 2020; Reimann et al., 2020).

The fluorescence microscopy showed results in two kinds of images. In the green-blue images, green represents microalgae and other phototrophs, whereas blue represents biomass visualized by DAPI + CW and their cellular polysaccharides. For the red-green images, red represents dead cells and live cells are dyed green.

2.4. Microscopic analysis and image processing

The morphology of the developed biofilms over LDPE and glass substrates was inspected using a field emission scanning electron microscope (JSM-7500F, Jeol, Tokyo, Japan). The micro-slides of biofilms on different substrates were prepared by immobilization using 2.5% glutaraldehyde in phosphate buffer (pH 7). Subsequently, serial dehydration with increasing ethanol volumes (10 min incubation duration) was performed using 50%, 75%, 90%, and 100% ethanol solutions. The samples went through a platinum coating in a deep vacuum for better perceptibility and were inspected using a semi-in-lens detector equipped with a gentle beam. The slides were observed at 5.00 kV accelerating voltage, × 250–550 magnification, and a working distance of 8 mm.

A Zeiss LSM 700 AxioObserver CLSM was used with Zeiss Zen 2012 software (Carl Zeiss, Oberkochen, Germany). A C-Apochromat objective (40×/1.20 W Korr M27) was used to capture digital images (512 × 512 pixels, 8 bit) at × 40 magnification. The cover glass thickness was 0.17 mm. The argon lasers and filter wavelengths for each channel are represented hereby; SYTO®9 (laser 488 nm, filter BP 490–555 nm), propidium iodide (laser 555 nm, filter 585–1000 nm), *Chlorophyll a* (laser 639 nm, filter 0–1000 nm), Calcofluor white + DAPI (laser 405 nm, filter 400–500 nm). An MBS 405/488/555/639 beam splitter was used along with a PMT detector (Tarafdar et al., 2022). After the CLSM adjustment settings were optimized, the same setup was kept throughout all scanning of the test series. We collected each image as a Z-Stack series through the thickness of the sample with distances among slices ranging from 2 to 5 μm, and there were 25–35 slices (focal planes) per image. Maximum intensity orthogonal projection was applied to flatten the image for the sake of 2-D visualization. As per the scheme of the experimental setup (Fig. S2, Supplementary Material), we had a total of 24 samples, *i.e.,* (pristine LDPE + LDPE with UV-327 + LDPE with UV-531 + glass substrate for 1 week in freshwater) × 3 sets and (pristine LDPE + LDPE with UV-327 + LDPE with UV-531 + glass substrate for 4 weeks in freshwater) × 3 sets. Biofilms are characterized by patchiness and non-homogeneous adhesion to the substratum. Therefore, for each of those 24 samples (4 samples × 2 durations × 3 sets), an area from the approximate midpart of sample fibers was selected randomly to take the images.

Volumetric measurements of the biofilms were obtained by BiofilmQ 0.2.2 (Drescher lab, Max Planck Institute for Terrestrial Microbiology, Marburg, Germany) using threshold-based 3D segmentation of the confocal images (Hartmann et al., 2021). The CLSM instrument generated '.czi' files were processed using BiofilmQ software to calculate biovolume for each fluorescence channel. The images were denoised by convolution. Top-Hat filtering was applied to remove background fluorescence and fluorescence between cells. The thresholding method applied was Ridler-Calvard (Ridler and Calvard, 1978) (sensitivity 0.09) and the cube dissection method (cube side length 20) was used for objects declumping. Global biofilm volume was selected as an object parameter to calculate total biofilm volume. Percentage differences between specific endpoints for the different samples were calculated based on the mean of the values from triplicate studies. Nonparametric Kruskal–Wallis one-way analysis of variance was conducted to test multiple comparisons statistically, and values of $p < 0.05$ were considered significant.

2.5. Test for oxidative stress

Earlier observations suggest that exposure to sublethal or subinhibitory oxidative stress can remarkably improve the formation and strength of biofilm (Dhakal et al., 2019; Villa et al., 2012). Based on this concept, we hypothesized that the reason for the formation of thicker biofilms on LDPE with UV stabilizers may reside in the possible generation of oxidative stress by the UV stabilizers.

The radical scavenging activity of the UV stabilizers was confirmed using the reactive oxygen species (ROS) sensitive reagent CellROX® Green. Freshly made 250 mL of LB broth was inoculated with 1 mL of freshwater collected from the previously mentioned sampling site. Pristine LDPE (control) and LDPE with both UV stabilizers containing varying mass fractions (0.3%, 1%, and 3% w/w) were added in separate flasks. The cultures were incubated for 48 h at 30 °C and thereafter LDPE fibers were collected. The experiment was conducted in triplicates. The fresh biofilms on the LDPE fibers were undergone CellROX® Green reagent (5 μL, ex/em: 485/520) treatment and incubated for 30 min at 37 °C. The fibers were consequently washed with PBS, dyed with Hoescht 33342 (1 μg mL^{-1}, ex/em: 340/510 nm), and incubated for 15 min before microscopy. Hoechst 33342 (2'-[4-ethoxyphenyl]-5-[4-methyl-1-piperazinyl]-2,5′-bi-1H-benzimidazole trihydrochloride trihydrate) is a cell-permeable DNA stain which binds to the AT-rich regions in the minor groove of double-stranded DNA. This arrangement helped to visualize stressed cells in green (CellROX® Green) and non-stressed cells in blue (Hoescht 33342) fluorescence. A negative control without CellROX® Green was checked for autofluorescence in the same excitation and emission range. Zeiss LSM 700 AxioObserver CLSM was used to take the microscopic images as Z-Stack series through the thickness of the sample. Maximum intensity orthogonal projection was used for 2-D visualization. Quantification of biofilm volume was conducted using BiofilmQ software as mentioned earlier.

2.6. Surface adhesion force measurement

AFM can be used to estimate the adhesion forces of materials, by studying the attraction between the atoms of a surface and an AFM probe (Jiang and Turner, 2016). Adhesion forces exhibited by the three fibers (pristine LDPE, LDPE with UV-327, and LDPE with UV-531) on a silicon tip were tested using the PinPoint™ Nanomechanical mode of Park-NX12 AFM (Park Systems, Seoul, Republic of Korea). Unmodified silicon tips are very appropriate concerning their capability to differentiate and recognize changes in polarity on a material surface (Colson et al., 2017). Contact mode images were taken with a scan rate of 0.13–0.14 Hz. The scan size was $10 \times 10\ \mu m^2$ and the resolution was 256 points × 256 lines. Topography images were handled by XEI data processing and analysis software (version 5.1.4) by Park Systems.

3. Results and discussion

3.1. UV stabilizers endorse early development of biofilms

3.1.1. The FESEM observation

Fig. 1 depicts a lower amount of cells on pristine LDPE fibers rather than on LDPE fibers with UV stabilizers and glass after one week. The pristine LDPE fiber was only partially inhabited by freshwater microbes (Fig. 1 a), whereas LDPE fibers with UV stabilizers were densely populated by microorganisms (Fig. 1 b-c). Along with the higher number of microorganisms, extracellular polymeric substances (EPS) produced and secreted by the biomass, assisted to make the comparatively condensed structure of the biofilms on LDPE fibers with UV stabilizers. EPS layer can resist chemical stressors (Ahn et al., 2016) and the production of EPS can be regulated via quorum sensing (Fones and Preston, 2012). Quorum sensing mutants of a microbial population may have a preference under oxidative stress (George et al., 2019). This observation hints

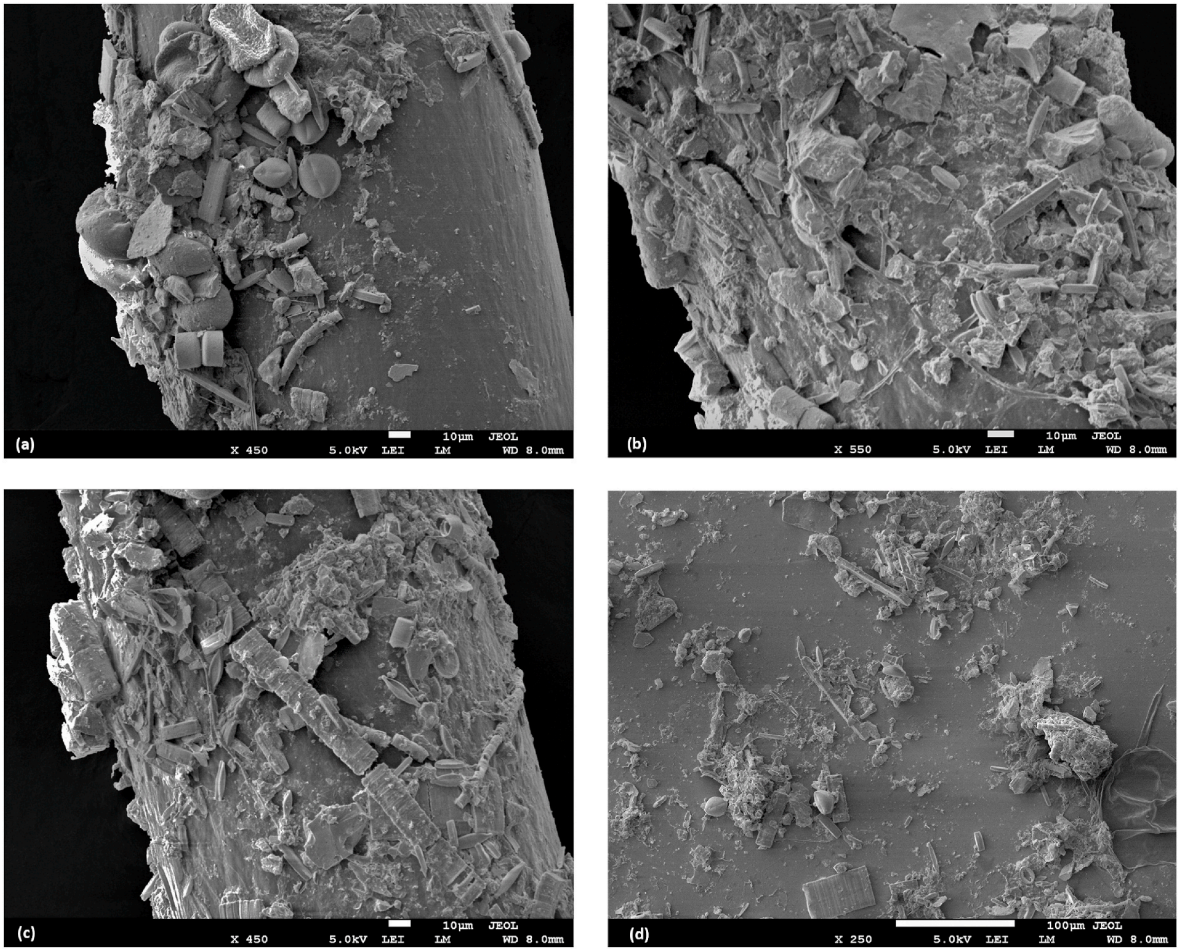

Fig. 1. FESEM images of one-week growth of plastisphere on different substrates, biofilm on (a) pristine LDPE, (b) LDPE with UV-327, (c) LDPE with UV-531, and (d) glass.

that the UV stabilizers may have generated oxidative stress which may eventually have influenced the development of EPSs to adjust to ominous environmental circumstances. The finding from FESEM can be confirmed by the CLSM results and test for oxidative stress.

3.1.2. *Chl-a autofluorescence and biomass visualized by DAPI + CW staining*

Images from staining using DAPI + CW and *Chl-a* autofluorescence suggest that, after the first week of the study, DAPI + CW visualized biofilm volumes were significantly higher on LDPE with UV-327, in comparison with pristine LDPE fibers (159% higher, Kruskal–Wallis test *p*-value 0.0315, Table S2, Supplementary Material) (Fig. 2 a, b & i). LDPE with UV-531 also showed a 33% increment in DAPI + CW visualized biovolume than that of the pristine LDPE (Fig. 2 a, c & i). Phototrophs (*Chl-a*) were prominently less on the pristine LDPE as there were 510%, 184%, and 634% higher *Chl-a* volumes in LDPE with UV-327, LDPE with UV-531 and glass substrate (Kruskal–Wallis test *p*-value < 0.05 for LDPE with UV327 and glass substrate). Plastic particles were previously studied to affect microalgal photosynthesis and growth (Sjollema et al., 2016; Wu et al., 2019). Thus, among glass substrate and pristine LDPE, the presence of fewer phototrophs on pristine LDPE was normal. However, higher phototroph volumes on LDPE with UV stabilizers compared to pristine LDPE were observed. UV stabilizers in LDPE may have boosted and/or accelerated the phototrophic growth on microplastics. The reason for this pattern of phototrophic microbial growth on different substrates can be hidden inside the sequential order of microbial colonization on plastic substrates. To develop a plastisphere biofilm, microorganisms first colonize the hydrophobic microplastic surfaces. Microbes, that are found to colonize microplastic surfaces in the earliest stage, are often reported as the class of γ- and α-proteobacteria (De Tender et al., 2017; Meyer-Cifuentes et al., 2020). According to a recent study by Latva et al. (2022), Bacteroidetes were observed to be most of the pioneer colonizers of microplastics, firstly followed by γ-proteobacteria and thereafter α-proteobacteria. Pioneer species of microbial colonization of microplastics may belong to other bacteria phyla like Actinobacteria (Didier et al., 2017) depending on different factors, *i.e.*, salinity, biogeography, plastic types, etc. This quick colonization is thereafter followed by *Chl-a* phototrophic organisms like members belonging to the Eukaryotic phylum Ochrophyta (*i.e.,* diatoms and brown algae), cyanobacteria, and green algae (Amaral-Zettler et al., 2021; Du et al., 2022; Latva et al., 2022). We can observe early colonization and higher density of pennate diatoms on LDPE with UV stabilizers in our study (Fig. S3, Supplementary Material). Diatoms are generally reported to colonize at the early stages of the development of various aquatic biofilms (Caruso, 2020; Sullivan, 2019) and this can be a reason behind high phototrophic biovolume on the glass substrate. (EPS

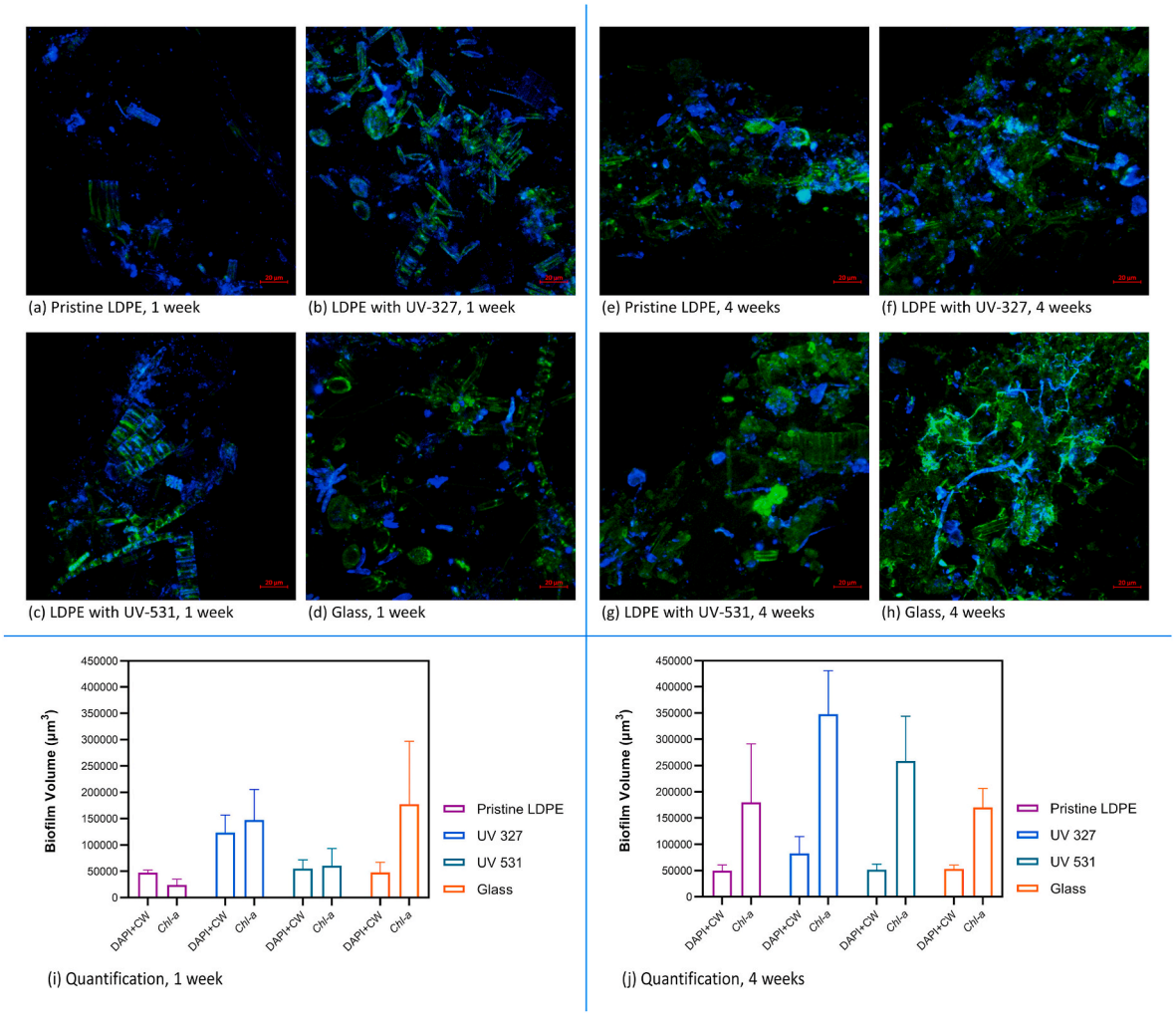

Fig. 2. (a–d) One-week growth of plastisphere on different substrates, **(e–h)** four weeks of plastisphere growth. Green represents microalgae and other phototrophs, blue represents biomass visualized by DAPI + CW (nucleic acids and cellular polysaccharides) [Set 2 and 3 are included in Fig. S4, Supplementary Material]. **(i & j)** Biovolume quantification of the plastisphere (one and four weeks of growth, respectively) on different substrates using BiofilmQ. Bars represent mean values of the triplicate biovolume quantification, and the error bars represent standard deviations. DAPI + CW stands for blue (biomass visualized by DAPI + CW) and *Chl-a* for green (autotrophs) fluorescence. (For interpretation of the references to colour in this figure legend, the reader is referred to the Web version of this article.)

secreted by these primary colonizers helps later stages biofilm colonizers to develop the secondary biofilm, which can take several months. The interest of our study is limited to only primary biofilm formation. Quantification-characterization of the EPS and the secondary biofilms can be a future endeavor.) Our observation suggests that UV stabilizers may have helped to speed up the process of primary biofilm development, as *Chl-a* phototroph biovolume was more on LDPE with UV stabilizers and very low on pristine LDPE. Thus, after one week of biofilm growth on pristine LDPE, there may be still non-*Chl-a* γ- and α-proteobacteria, Bacteroidetes, while diatoms and cyanobacteria may have already colonized LDPE with UV stabilizers. Further biomolecular analysis like Fluorescence In Situ Hybridization (FISH) is needed to confirm this phenomenon in future studies. It is worth mentioning, that γ- and α-proteobacteria may contain bacteriochlorophylls, but they have different fluorescence properties from *Chl-a* (Grimm et al., 2006).

After four weeks of biofilm growth (Fig. 2 e-h & j), we observed no statistically significant differences between biovolumes on pristine LDPE and glass (Table S2, Supplementary Material), but the DAPI + CW biovolumes on LDPE with UV-327 were marginally higher on the fourth week (66% and 57% higher than pristine LDPE and glass). *Chl-a* phototrophs colonized pristine LDPE after a month of biofilm development. Yet, *Chl-a* biovolumes for LDPE with UV-327 were 93% and 104% higher than pristine LDPE and glass substrate; for LDPE with UV-531, *Chl-a* biovolumes were 44% and 52% higher than pristine LDPE and glass substrate. The higher adherence property of LDPE with UV stabilizers might have helped to maintain the higher biovolume. Both UV-327 and UV-531 have a phenolic group that contributes to hydrogen bonding. Thus, intermolecular forces at the surfaces of LDPE particles with UV stabilizers should be stronger than that of the pristine LDPE, which can favor the adherence of microbial wall polysaccharides. Earlier, Zhao et al. (2021) found higher proportions of phototrophs (*Chl-a*) in the first week of biofilm growth compared to that of eight weeks (*in situ* study in marine water with commercial PE, PP, and PS as substrate). This depletion of phototrophs after the second month of the study likely occurred due to the adhesion of secondary biofilm colonizers (Schlundt et al., 2020; Wright et al., 2020). In our case, the developed biofilm probably did not enter the secondary phase in the period of four weeks, and that is the reason for the high phototroph abundance in the plastisphere. No notable variation of proportional phototrophic biovolumes was found on the glass substrate between the first and fourth week of the study.

3.1.3. *Visualization of live-dead cells*

Fig. 3 shows that pristine LDPE had the least of all biovolumes in the first week (Kruskal–Wallis test p-value < 0.05) (Fig. 3a and i). Although LDPE with UV stabilizers had a similar total biovolume as the glass

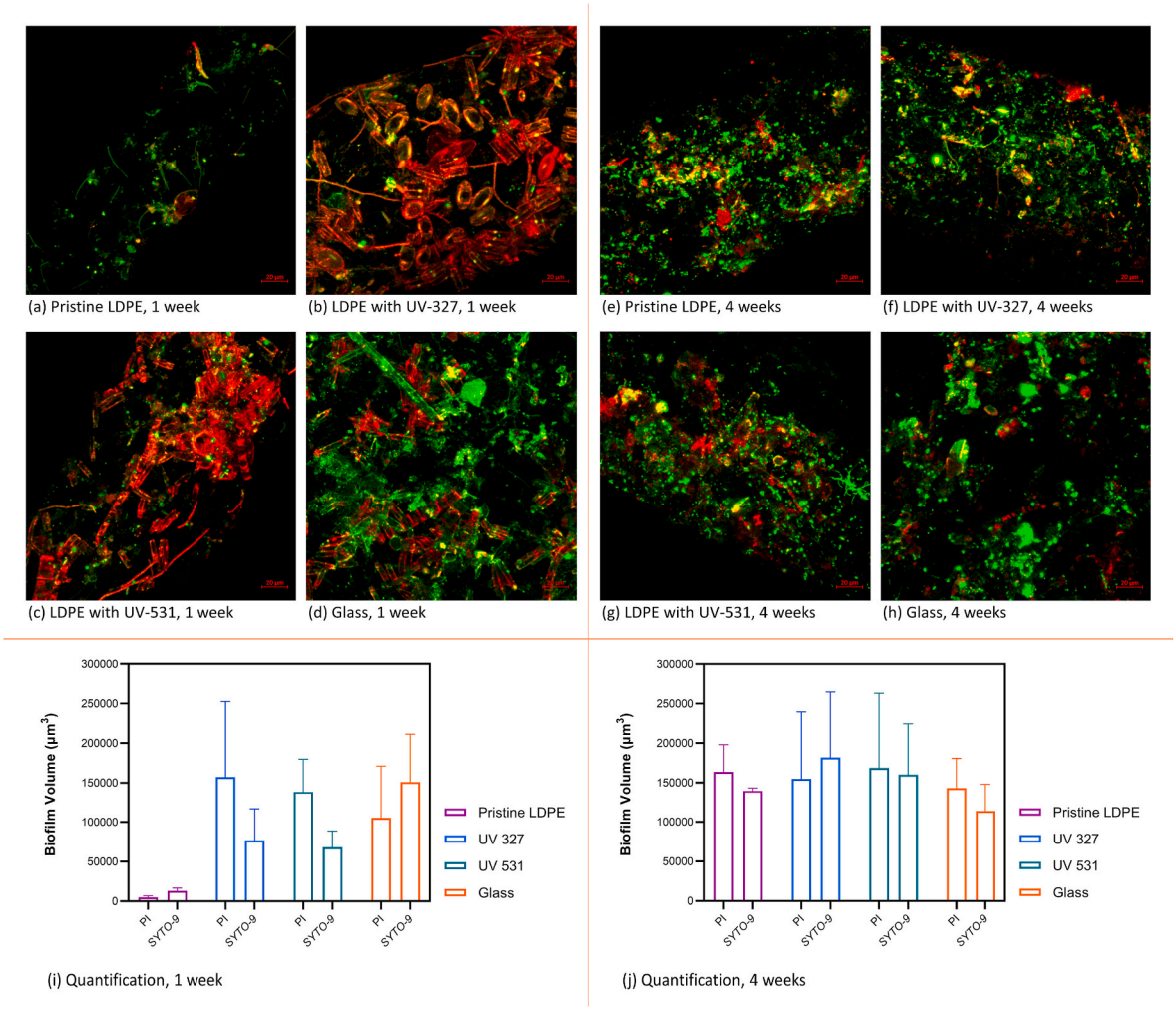

Fig. 3. **(a–d)** One-week growth of plastisphere on different substrates, **(e–h)** four weeks of plastisphere growth. Green represents live cells and red represents dead cells [Set 2 & 3 are included in Fig. S5, Supplementary Material]. **(i & j)** Biovolume measurement of the plastisphere (one and four weeks of growth, respectively) on different substrates using BiofilmQ. Bars represent mean values of the triplicate biovolume quantification, and the error bars represent standard deviations. PI stands for red (dead) and SYTO-9 stands for green (alive) fluorescence. (For interpretation of the references to colour in this figure legend, the reader is referred to the Web version of this article.)

substrate, the cells were mostly dead, likely due to the toxicity of UV stabilizers (104% and 103% higher dead biovolume than live biovolume in LDPE with UV-327 and LDPE with UV-531; whereas 43% higher live biovolume in glass substrate) (Fig. 3 b-d & i). Unsurprisingly, the small biovolume on pristine LDPE was mostly alive (171% higher live biovolume compared to the dead biovolume). In comparison to pristine LDPE, there was a significantly higher biovolume of dead cells present on LDPE with UV stabilizers (Kruskal–Wallis test p-value < 0.05).

At the end of the four-week growth period, similar amounts of total biovolume were observed, with marginally higher biovolumes for substrates with UV stabilizers (LDPE with UV-327 was 31% and 11% higher than glass and pristine LDPE; LDPE with UV-531 was 28% and 8.5%% higher than glass and pristine LDPE) (Fig. 3 e-h & j). Biofilms on LDPE with UV stabilizers possessed a significant increment in the alive cells biovolumes from the observation of the first week (Kruskal–Wallis test p-value 0.0062; 136% higher alive biovolume for LDPE with UV-327 and 135% higher for LDPE with UV-531). This revival of biofilm may be occurred because of the reformation of the biofilm upon dead bacterial cells (Wang et al., 2019). Contact-active antimicrobial surfaces are repeatedly found to get self-deactivated by the surface-adhered sufficiently thick bacterial dead layer, which protects incoming bacteria from the surface antimicrobial activity (Cloutier et al., 2015; Riga et al., 2017; Siedenbiedel and Tiller, 2012). Taheri-Araghi and Guerbidjian (2020) explained that the dead layer of peripheral cells of a biofilm can safeguard internal cells by obstructing antimicrobial peptide flux. Thus, the dead biofilm layer can hinder the leaching out of UV stabilizers and the upper layer of bacteria cannot even 'see' the microplastic surface (Wright et al., 2020). This phenomenon is similar to the findings of our previous study, where biofilm development occurred on top of a protective layer of already dead microorganisms (Tarafdar et al., 2018). The effect of the biofilm on the leaching attributes of microplastics can be a seed for subsequent studies. A remarkably decreased overall cell size of

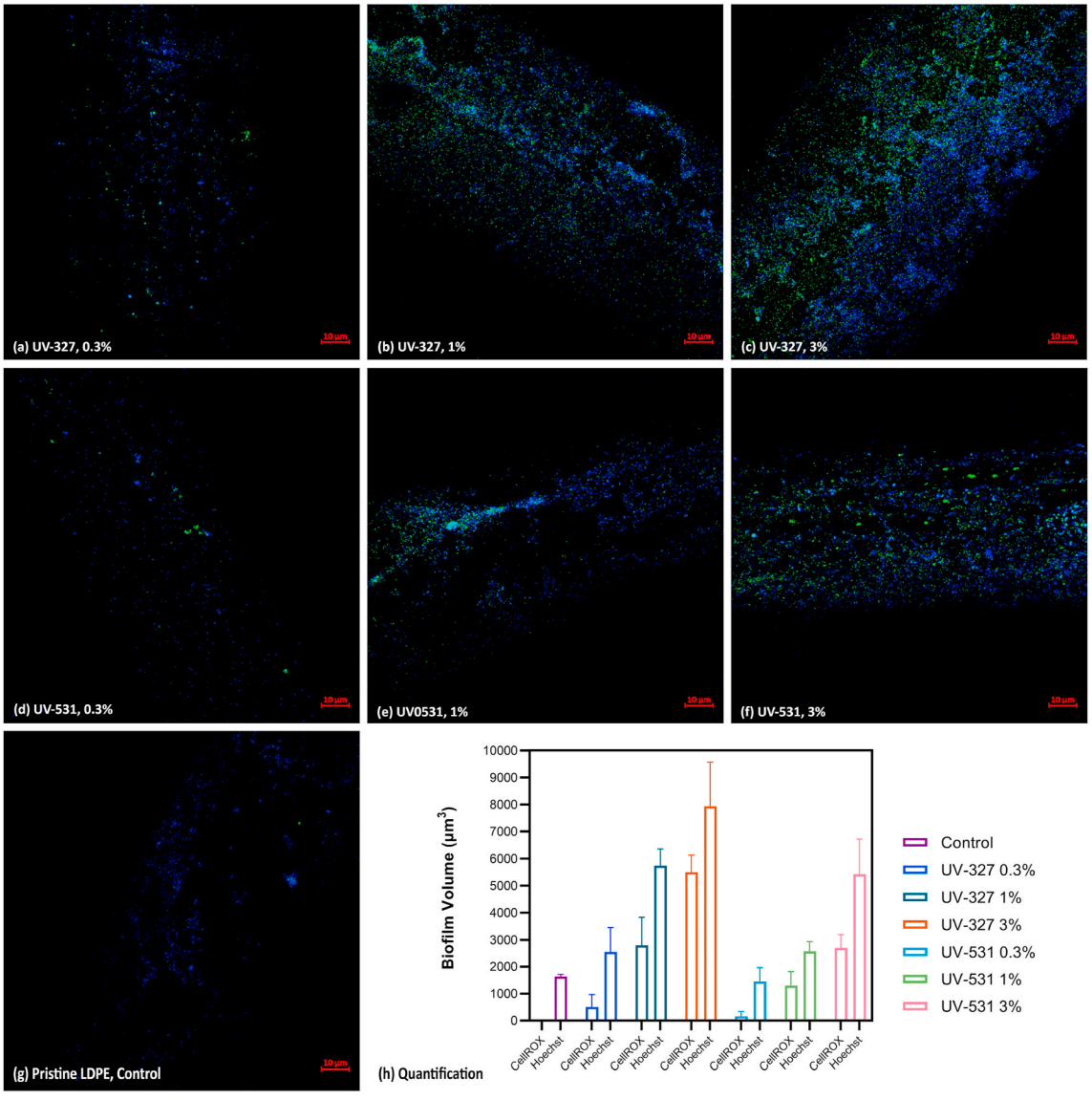

Fig. 4. Radical scavenging activities of the UV stabilizers are confirmed using the ROS-sensitive reagent CellROX® Green. Two-days-old thin biofilm on **(a)** LDPE with 0.3% (w/w) UV-327, **(b)** LDPE with 1% (w/w) UV-327, **(c)** LDPE with 3% (w/w) UV-327, **(d)** LDPE with 0.3% (w/w) UV-531, **(e)** LDPE with 1% (w/w) UV-531, **(f)** LDPE with 3% (w/w) UV-531, **(g)** pristine LDPE without UV stabilizers. Blue fluorescence (Hoechst 33342) signifies un-stressed cells and green fluorescence (CellROX®) signifies oxidative stressed cells [Set 2 & 3 are included in Fig. S7, Supplementary Material]. **(h)** Biovolume measurement of the plastisphere on different substrates using BiofilmQ after 2-days of biofilm growth. Bars represent mean values of the triplicate biovolume quantification, and the error bars represent standard deviations. CellROX stands for green (stressed), and Hoechst stands for blue (non-stressed) fluorescence. (For interpretation of the references to colour in this figure legend, the reader is referred to the Web version of this article.)

the biofilms was also observed in the fourth week. This is consistent with previous reports where cell size became smaller with longer growth periods (Schlundt et al., 2020; Zhao et al., 2021).

3.2. Biofilm endorsement of UV stabilizers can be linked to oxidative stress

Oxidative stress is an increased intracellular levels of ROS that can result in damage to lipids, proteins, and nucleic acids (Schieber and Chandel, 2014). Oxidative stress study indicated that in a lower mass fraction of UV stabilizers (0.3% w/w) the biofilm volume (Fig. 4 a & d) was close to the biofilm volume on pristine LDPE (Fig. 4 g). The presence of oxidative stressed cells became visible in the biofilm, even with the lowest mass fraction (0.3% w/w) of UV stabilizers. The total volume of the biofilm increased with the increasing mass fraction of UV stabilizers in the LDPE fiber. Simultaneously, the biovolume of the stressed cells also increased with the increasing mass fraction of UV stabilizers (Fig. 4). The ratio of stressed to non-stressed cells increased with increasing mass fraction for both the UV stabilizers in LDPE fiber (Fig. S6, Supplementary Material). The volumes of both stressed and total cells were higher in the fibers with UV-327 in comparison with UV-531. Higher biovolumes (39%) for UV-327 than UV-531 were also observed in the previous experiment conducted in the freshwater stream. UV-327 generated more oxidative stress (205%, 116%, and 103% higher for 0.3%, 1%, and 3% w/w added UV stabilizers) on the biofilm cells than UV-531 (Fig. 4 h), which was likely chlorine-induced oxidative stress due to the presence of the chlorine atom (Dhakal et al., 2019) on the surface of LDPE with UV-327 (Fig. S8, Supplementary Material). This explains why the total biovolume and volume of stressed cells, both on LDPE with UV-327 were even higher than on LDPE with UV-531.

Earlier, benzotriazole UV stabilizers were reported to cause dysfunction in mitochondrial bioenergetics and induce oxidative stress in developing zebrafish (Liang et al., 2019). Giraudo et al. (2017) observed that benzotriazole UV stabilizers like UV-234 and UV-328 can elevate ROS generation along with oxidative stress related genes (*i.e.,* glutathione peroxidase, superoxide dismutase, and catalase) in freshwater green algae *Chlamydomonas reinhardtii.* ROS can cause an effect of hormesis on microbial growth. At higher concentrations it is unfavorable to microbes, as they can cause reactions with crucial biological molecules; yet at lower concentrations ROS can promote signal transduction and shifting of metabolic pathways, resulting in induced microbial development and beefier biofilms (Gambino and Cappitelli, 2016; Wang et al., 2022a). Earlier studies reported that oxidative stress can effectively stimulate the growth of biofilms (Oh et al., 2016; Wang et al., 2020a). The reason can be the mechanism of quorum sensing. It is a central system of chemical-signal-based communication among bacterial cells in a community, which can regulate the characteristic behavior of bacteria, as-well-as biofilm. The contribution of this communication is to balance the performance of cells, secure nutrients, cell mobility, secretion of secondary metabolites, and enhance gene transfer among the cells (Preda and Săndulescu, 2019). Another report suggests that mutants with quorum sensing can be favored while a bacterial population is under oxidative stress (George et al., 2019). The quorum sensing process can be directly linked to the formation and enhancement of biofilms (Chen et al., 2022; Mukherjee et al., 2019).

3.3. Surface adhesion force

Fig. 5 a-c depicts the AFM PinPoint™ Nanomechanical mode generated adhesion force distribution topology images, measured between silicon probe and the three types of fibers (pristine LDPE, LDPE

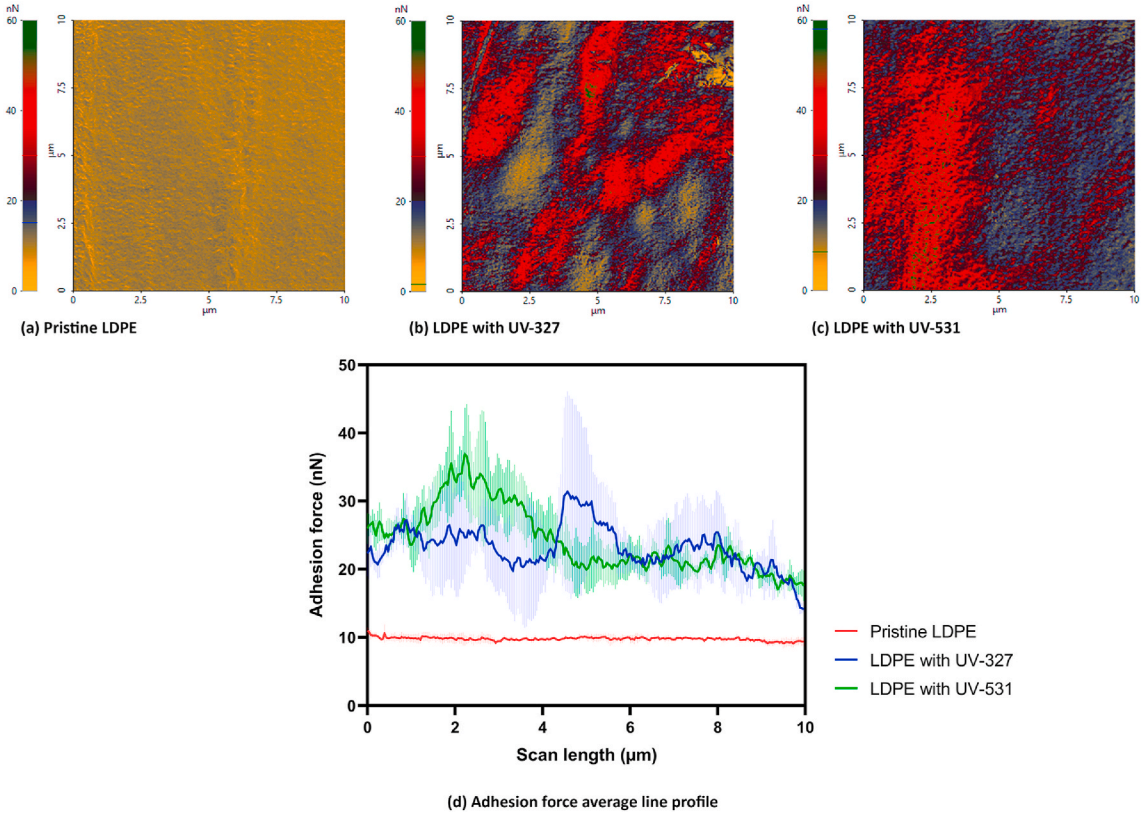

Fig. 5. AFM PinPoint™ Nanomechanical mode generated adhesion force distribution topology image. Measurement between silicon probe and (a) pristine LDPE, (b) LDPE with UV-327, (c) LDPE with UV-531. (d) Adhesion force line profile of pristine LDPE, LDPE with UV-327 (1% w/w), and LDPE with UV-531 (1% w/w). Lines represent the mean values of triplicate adhesion data and error bars represent the standard deviations. (For interpretation of the references to colour in this figure legend, the reader is referred to the Web version of this article.)

with UV-327 & LDPE with UV-531). Average line profiles of measured adhesion forces (triplicate data) are provided in Fig. 5 d. LDPE with UV stabilizers possessed consistently stronger adhesion force compared to the pristine LDPE. LDPE with UV-327 had 136% and LDPE with UV-531 had 148% higher adhesion force than that of the pristine LDPE. These elevated adhesion forces on the surfaces of LDPE with UV stabilizers probably boosted the initial microbial attachment, resulting in the speedy development of primary biofilm. Energy dispersive X-Ray composition analysis (Fig. S8, Supplementary Material) showed the presence of chlorine atoms only on the surface of LDPE with UV-327 (0.40% w/w). Chlorine substitution at the surface of LDPE may allow polar van der Waals interactions with microbial bodies in addition to the hydrogen bonding of phenolic groups both in UV-327 and UV-531. The presence of these chlorine atoms can contribute to chlorine-induced oxidative stress, which eventually resulted in more ROS generation in biofilms on LDPE with UV-327 surface than that of the LDPE with UV-531. Boosted amount of oxygen atoms on the surface of LDPE with UV-531 (10.04% w/w) can be explained by the ketone and phenolic groups in the molecule. Surface roughness of the three kinds of fibers did not seem to be affected noticeably with the incorporation of UV stabilizers (Fig. S9, Supplementary Material), which denotes no role of surface roughness property on the boosted biofilm development on LDPE with UV stabilizers.

3.4. Environmental implications

Biofilms occasionally respond to antimicrobial compounds below the fatal dose with enhanced microbial signaling, resource allocation efficacy, and EPS synthesis to protect microorganisms from harmful chemicals. This can protect the biofilm from environmental stressors (Gambino and Cappitelli, 2016). Specifically in this study, the toxic effects and higher adhesivity due to UV stabilizers are observed to boost the biofilm volume quicker than the biofilm on LDPE without UV stabilizers.

This increase in biofilm resilience may occur in a variety of wastewater that comprises biohazardous hospital wastes (Wang et al., 2022a). Being persistent in the aquatic environment, microplastics possess a higher tendency to act as a vector of pathogenic microbes (Bowley et al., 2021). Recent reports have already shown that pathogens can populate and grow in biofilms on oceanic microplastic debris (Di Pippo et al., 2020; Kaur et al., 2022; Kirstein et al., 2016; Pham et al., 2021; Shi et al., 2021). ARGs [*i.e.*, sul1, erm(B), intI1, and intI2] were observed to be elevated on microplastic biofilms compared to the surrounding water (Mughini-Gras et al., 2021;Wang et al., 2020). Arias-Andres et al. (2018) studied the plasmid transfer and gene exchange in microplastics-contaminated oceanic biological systems and concluded that biofilms on plastic surfaces can furnish unconventional hotspot areas for outspreading and proliferation of ARGs by horizontal gene transfer.

Therefore, in an aquatic environment receiving hospital waste pathogens, UV stabilizers might elevate the volume of plastisphere pathogens and ARGs, resulting in decreased efficiency of pathogen removal strategies. On the other hand, the quick development of biofilms tends to increase the density of buoyant microplastics, thereby transporting them to sediments (Lee et al., 2022; Semcesen and Wells, 2021). Boosted development of biofilms can also complicate the removal of microplastics in WWTP by changing the surface characteristics (Carr et al., 2016).

4. Conclusions

LDPEs with UV stabilizers exhibited considerably stronger surface adhesion force, contrasted with the pristine LDPE. The increased adsorption capability of LDPEs with UV stabilizers containing polar functional groups can help to attach early colonizer microbes to the microplastic surface, during the primary biofilm developmental phase. Although the early colonizers were killed owing to the toxicity of UV stabilizers, the dead biofilm layer mitigated the toxicity. Subsequently, new microbes can grow on the dead biofilm layer without getting much affected by the toxicity. The slower release of UV stabilizers from LDPE due to the additional mass transfer barrier (Do et al., 2022) would explain the mitigated toxic effects. UV stabilizers also induced microorganismic intracellular ROS and this oxidative stress can favor the quorum sensing mutants which ultimately results in thicker biofilm development. In combination, the toxic effects and higher adhesivity due to UV stabilizers are observed to boost the biofilm volume quicker than the biofilm on LDPE without UV stabilizers, ultimately resulting in the overall early development of biofilms on plastics. Further studies on the effects of additives on the variation of the microbial community are required to extend our understanding of developing biofilms on microplastics of diverse origins.

Credit author statement

Abhrajyoti Tarafdar: Conceptualization; Data curation; Formal analysis; Funding acquisition; Investigation; Methodology; Project administration; Software; Validation; Visualization; Roles/Writing - original draft.; **Ja-yun Lim**: Methodology; Resources; Software.; **Jung-Hwan Kwon:** Supervision; Project administration; Validation; Visualization; Writing - review & editing; Resources; Funding acquisition.

Declaration of competing interest

The authors declare the following financial interests/personal relationships which may be considered as potential competing interests: Abhrajyoti Tarafdar reports financial support was provided by National Research Foundation of Korea (NRF).

Data availability

Data will be made available on request.

Acknowledgments

This work was supported by the National Research Foundation of Korea (NRF) grants funded by the Korean government (MEST) [grant numbers 2020R1A2C2009244 & 2021R1I1A1A01059838]. The authors would like to acknowledge Dr. Anh T. N. Do, Division of Environmental Science and Ecological Engineering, Korea University, for helping in the manufacturing process of plastic fibers. The authors also thank Editage for providing language editing guidance.

Appendix A. Supplementary data

Supplementary data to this article can be found online at https://doi.org/10.1016/j.envpol.2022.120444.

References

Ahn, S., Jung, J., Jang, I.A., Madsen, E.L., Park, W., 2016. Role of glyoxylate shunt in oxidative stress response. J. Biol. Chem. 291, 11928–11938. https://doi.org/10.1074/jbc.M115.708149.

Amaral-Zettler, L.A., Zettler, E.R., Mincer, T.J., Klaassen, M.A., Gallager, S.M., 2021. Biofouling impacts on polyethylene density and sinking in coastal waters: a macro/micro tipping point? Water Res. 201, 117289 https://doi.org/10.1016/j.watres.2021.117289.

Arias-Andres, M., Klümper, U., Rojas-Jimenez, K., Grossart, H.P., 2018. Microplastic pollution increases gene exchange in aquatic ecosystems. Environ. Pollut. 237, 253–261. https://doi.org/10.1016/j.envpol.2018.02.058.

Bowley, J., Baker-Austin, C., Porter, A., Hartnell, R., Lewis, C., 2021. Oceanic hitchhikers – assessing pathogen risks from marine microplastic. Trends Microbiol. 29, 107–116. https://doi.org/10.1016/J.TIM.2020.06.011.

Cai, L., Wu, D., Xia, J., Shi, H., Kim, H., 2019. Influence of physicochemical surface properties on the adhesion of bacteria onto four types of plastics. Sci. Total Environ. 671, 1101–1107. https://doi.org/10.1016/j.scitotenv.2019.03.434.

Cai, H., Liang, J., Ning, X. an, Lai, X., Li, Y., 2020. Algal toxicity induced by effluents from textile-dyeing wastewater treatment plants. J. Environ. Sci. (China) 91, 199–208. https://doi.org/10.1016/j.jes.2020.01.004.
Carr, S.A., Liu, J., Tesoro, A.G., 2016. Transport and fate of microplastic particles in wastewater treatment plants. Water Res. 91, 174–182. https://doi.org/10.1016/J.WATRES.2016.01.002.
Caruso, G., 2020. Microbial colonization in marine environments: overview of current knowledge and emerging research topics, 2020 J. Mar. Sci. Eng. 8, 78. https://doi.org/10.3390/JMSE8020078, 8, 78.
Chen, M., Cai, Y., Li, G., Zhao, H., An, T., 2022. The stress response mechanisms of biofilm formation under sub-lethal photocatalysis. Appl. Catal. B Environ. 307, 121200 https://doi.org/10.1016/j.apcatb.2022.121200.
Cloutier, M., Mantovani, D., Rosei, F., 2015. Antibacterial coatings: challenges, perspectives, and opportunities. Trends Biotechnol. 33, 637–652. https://doi.org/10.1016/J.TIBTECH.2015.09.002.
Colson, J., Andorfer, L., Nypelö, T.E., Lütkemeier, B., Stöckel, F., Konnerth, J., 2017. Comparison of silicon and OH-modified AFM tips for adhesion force analysis on functionalised surfaces and natural polymers. Colloids Surfaces A Physicochem. Eng. Asp. 529, 363–372. https://doi.org/10.1016/J.COLSURFA.2017.06.017.
Darrene, L.-N., Cecile, B., 2016. Experimental models of oral biofilms developed on inert substrates: a review of the literature. https://doi.org/10.1155/2016/7461047.
Davidov, K., Iankelevich-Kounio, E., Yakovenko, I., Koucherov, Y., Rubin-Blum, M., Oren, M., 2020. Identification of plastic-associated species in the mediterranean sea using DNA metabarcoding with nanopore MinION. Sci. Rep. 10, 1–11. https://doi.org/10.1038/s41598-020-74180-z.
de Carvalho, A.R., Riem-Galliano, L., ter Halle, A., Cucherousset, J., 2022. Interactive effect of urbanization and flood in modulating microplastic pollution in rivers. Environ. Pollut. 309, 119760 https://doi.org/10.1016/J.ENVPOL.2022.119760.
de Haan, W.P., Sanchez-Vidal, A., Canals, M., 2019. Floating microplastics and aggregate formation in the western mediterranean sea. Mar. Pollut. Bull. 140, 523–535. https://doi.org/10.1016/J.MARPOLBUL.2019.01.053.
De Tender, C., Devriese, L.I., Haegeman, A., Maes, S., Vangeyte, J., Cattrijsse, A., Dawyndt, P., Ruttink, T., 2017. Temporal dynamics of bacterial and fungal colonization on plastic debris in the north sea. Environ. Sci. Technol. 51, 7350–7360. https://doi.org/10.1021/acs.est.7b00697.
Devereux, R., Westhead, E.K., Jayaratne, R., Newport, D., 2022. Microplastic abundance in the thames river during the new year period. Mar. Pollut. Bull. 177, 113534 https://doi.org/10.1016/J.MARPOLBUL.2022.113534.
Dhakal, J., Sharma, C.S., Nannapaneni, R., McDaniel, C.D., Kim, T., Kiess, A., 2019. Effect of chlorine-induced sublethal oxidative stress on the biofilm-forming ability of *Salmonella* at different temperatures, nutrient conditions, and substrates. J. Food Protect. 82, 78–92. https://doi.org/10.4315/0362-028X.JFP-18-119.
Di Pippo, F., Venezia, C., Sighicelli, M., Pietrelli, L., Di Vito, S., Nuglio, S., Rossetti, S., 2020. Microplastic-associated biofilms in lentic Italian ecosystems. Water Res. 187, 116429 https://doi.org/10.1016/j.watres.2020.116429.
Didier, D., Anne, M., Alexandra, T.H., 2017. Plastics in the North Atlantic garbage patch: a boat-microbe for hitchhikers and plastic degraders. Sci. Total Environ. 599 (600), 1222–1232. https://doi.org/10.1016/j.scitotenv.2017.05.059.
Do, A.T.N., Ha, Y., Kang, H.J., Kim, J.M., Kwon, J.H., 2022. Equilibrium leaching of selected ultraviolet stabilizers from plastic products. J. Hazard Mater. https://doi.org/10.1016/j.jhazmat.2021.128144.
Du, Y., Liu, X., Dong, X., Yin, Z., 2022. A review on marine plastisphere: biodiversity, formation, and role in degradation. Comput. Struct. Biotechnol. J. https://doi.org/10.1016/j.csbj.2022.02.008.
ECHA, 2022a. Candidate list of substances of very high concern for authorisation [WWW Document] Eur. Chem. Agency. URL. https://echa.europa.eu/web/guest/candidate-list-table. accessed 8.26.22.
ECHA, 2022b. Substance evaluation - CoRAP [WWW document] Eur. Chem. Agency. URL. https://echa.europa.eu/information-on-chemicals/evaluation/community-rolling-action-plan/corap-table. accessed 4.1.22.
Fones, H., Preston, G.M., 2012. Reactive oxygen and oxidative stress tolerance in plant pathogenic *Pseudomonas*. FEMS Microbiol. Lett. 327, 1–8. https://doi.org/10.1111/J.1574-6968.2011.02449.X.
Gambino, M., Cappitelli, F., 2016. Mini-review: biofilm responses to oxidative stress. Biofouling. https://doi.org/10.1080/08927014.2015.1134515.
Gao, R., Sun, C., 2021. A marine bacterial community capable of degrading poly (ethylene terephthalate) and polyethylene. J. Hazard Mater. 416, 125928 https://doi.org/10.1016/j.jhazmat.2021.125928.
George, S.E., Hrubesch, J., Breuing, I., Vetter, N., Korn, N., Hennemann, K., Bleul, L., Willmann, M., Ebner, P., Götz, F., Wolz, C., 2019. Oxidative stress drives the selection of quorum sensing mutants in the *Staphylococcus aureus* population. Proc. Natl. Acad. Sci. U.S.A. 116, 19145–19154. https://doi.org/10.1073/pnas.1902752116.
Giraudo, M., Cottin, G., Esperanza, M., Gagnon, P., Silva, A.O.D., Houde, M., 2017. Transcriptional and cellular effects of benzotriazole UV stabilizers UV-234 and UV-328 in the freshwater invertebrates *Chlamydomonas reinhardtii* and *Daphnia magna*. Environ. Toxicol. Chem. 36, 3333–3342. https://doi.org/10.1002/ETC.3908.
Goff, J., Whelan, T., 2013. The Dynisco Extrusion Processors Handbook, second ed. DYNISCO.
Grimm, B., Porra, R.J., Ruediger, W., Scheer, H., 2006. Chlorophylls and Bacteriochlorophylls : Biochemistry, Biophysics, Functions and Applications. Springer, Dordrecht. https://doi.org/10.1007/1-4020-4516-6.
Hartmann, R., Jeckel, H., Jelli, E., Singh, P.K., Vaidya, S., Bayer, M., Rode, D.K.H., Vidakovic, L., Díaz-Pascual, F., Fong, J.C.N., Dragoš, A., Lamprecht, O., Thöming, J. G., Netter, N., Häussler, S., Nadell, C.D., Sourjik, V., Kovács, Á.T., Yildiz, F.H., Drescher, K., 2021. Quantitative image analysis of microbial communities with BiofilmQ. Nat. Microbiol. 6, 151–156. https://doi.org/10.1038/s41564-020-00817-4.
Hasegawa, T., Mizukawa, K., Yeo, B.G., Sekioka, T., Takada, H., Nakaoka, M., 2022. Trophic Transfer of Microplastics Enhances Plastic Additive Accumulation in Fish. https://doi.org/10.1101/2021.03.09.434685 bioRxiv 2021.03.09.434685.
Hu, W., Murata, K., Zhang, D., 2017. Applicability of LIVE/DEAD BacLight stain with glutaraldehyde fixation for the measurement of bacterial abundance and viability in rainwater. J. Environ. Sci. (China) 51, 202–213. https://doi.org/10.1016/j.jes.2016.05.030.
Huang, W., Song, B., Liang, J., Niu, Q., Zeng, G., Shen, M., Deng, J., Luo, Y., Wen, X., Zhang, Y., 2021. Microplastics and associated contaminants in the aquatic environment: a review on their ecotoxicological effects, trophic transfer, and potential impacts to human health. J. Hazard Mater. 405 https://doi.org/10.1016/J.JHAZMAT.2020.124187.
Intelligence, M., 2021. UV absorber market - growth, trends, Covid-19 impact, and forecasts (2022 - 2027) [WWW Document]. URL accessed 7.29.22. https://www.mordorintelligence.com/industry-reports/uv-absorber-market.
Jiang, Y., Turner, K.T., 2016. Measurement of the strength and range of adhesion using atomic force microscopy. Extrem. Mech. Lett. 9, 119–126. https://doi.org/10.1016/J.EML.2016.05.013.
Kaur, K., Reddy, S., Barathe, P., Oak, U., Shriram, V., Kharat, S.S., Govarthanan, M., Kumar, V., 2022. Microplastic-associated pathogens and antimicrobial resistance in environment. Chemosphere 291, 133005. https://doi.org/10.1016/J.CHEMOSPHERE.2021.133005.
Kirstein, I.V., Kirmizi, S., Wichels, A., Garin-Fernandez, A., Erler, R., Löder, M., Gerdts, G., 2016. Dangerous hitchhikers? Evidence for potentially pathogenic Vibrio spp. on microplastic particles. Mar. Environ. Res. 120, 1–8. https://doi.org/10.1016/J.MARENVRES.2016.07.004.
Latva, M., Dedman, C.J., Wright, R.J., Polin, M., Christie-Oleza, J.A., 2022. Microbial pioneers of plastic colonisation in coastal seawaters. Mar. Pollut. Bull. 179, 113701 https://doi.org/10.1016/J.MARPOLBUL.2022.113701.
Lee, S.-Y., An, J., Kim, J., Kwon, J.-H., 2022. Enhanced settling of microplastics after biofilm development: a laboratory column study mimicking wastewater clarifiers. Environ. Pollut. 311, 119909 https://doi.org/10.1016/J.ENVPOL.2022.119909.
Li, Z., Liang, X., Liu, W., Zhao, Y., Yang, H., Li, W., Adamovsky, O., Martyniuk, C.J., 2020. Elucidating mechanisms of immunotoxicity by benzotriazole ultraviolet stabilizers in zebrafish (*Danio rerio*): implication of the AHR-IL17/IL22 immune pathway. Environ. Pollut. 262, 114291 https://doi.org/10.1016/j.envpol.2020.114291.
Liang, X., Li, J., Martyniuk, C.J., Wang, J., Mao, Y., Lu, H., Zha, J., 2017. Benzotriazole ultraviolet stabilizers alter the expression of the thyroid hormone pathway in zebrafish (*Danio rerio*) embryos. Chemosphere 182, 22–30. https://doi.org/10.1016/j.chemosphere.2017.05.015.
Liang, X., Adamovsky, O., Souders, C.L., Martyniuk, C.J., 2019. Biological effects of the benzotriazole ultraviolet stabilizers UV-234 and UV-320 in early-staged zebrafish (*Danio rerio*). Environ. Pollut. 245, 272–281. https://doi.org/10.1016/j.envpol.2018.10.130.
Lin, Q.B., Liang, X.Z., Su, Q.Z., Shan, L.J., Wang, Z.W., 2017. Effect of graphene on the migration of two ultraviolet absorbents from graphene-LDPE composite films into a fatty food simulant. Food Packag. Shelf Life 12, 9–15. https://doi.org/10.1016/j.fpsl.2017.01.008.
Liu, Y., You, J.A., Li, Y.J., Zhang, J. Di, He, Y., Breider, F., Tao, S., Liu, W.X., 2021. Insights into the horizontal and vertical profiles of microplastics in a river emptying into the sea affected by intensive anthropogenic activities in Northern China. Sci. Total Environ. 779, 146589 https://doi.org/10.1016/J.SCITOTENV.2021.146589.
Markets and Markets, 2022. UV absorbers market global forecast to 2022 [WWW Document]. URL. https://www.marketsandmarkets.com/Market-Reports/uv-absorber-market-39452163.html. accessed 7.29.22.
Meyer-Cifuentes, I.E., Werner, J., Jehmlich, N., Will, S.E., Neumann-Schaal, M., Öztürk, B., 2020. Synergistic biodegradation of aromatic-aliphatic copolyester plastic by a marine microbial consortium. Nat. Commun. 11, 1–13. https://doi.org/10.1038/s41467-020-19583-2.
Miao, L., Gao, Y., Adyel, T.M., Huo, Z., Liu, Z., Wu, J., Hou, J., 2021a. Effects of biofilm colonization on the sinking of microplastics in three freshwater environments. J. Hazard Mater. 413, 125370 https://doi.org/10.1016/j.jhazmat.2021.125370.
Miao, L., Yu, Y., Adyel, T.M., Wang, C., Liu, Z., Liu, S., Huang, L., You, G., Meng, M., Qu, H., Hou, J., 2021b. Distinct microbial metabolic activities of biofilms colonizing microplastics in three freshwater ecosystems. J. Hazard Mater. 403, 123577 https://doi.org/10.1016/j.jhazmat.2020.123577.
Montecinos, S., Tognana, S., Pereyra, M., Silva, L., Tomba, J.P., 2020. Study of a Stream in Argentina with a High Concentration of Microplastics: Preliminary Analysis of the Methodology. https://doi.org/10.1016/j.scitotenv.2020.143390.
Mughini-Gras, L., van der Plaats, R.Q.J., van der Wielen, P.W.J.J., Bauerlein, P.S., de Roda Husman, A.M., 2021. Riverine microplastic and microbial community compositions: a field study in The Netherlands. Water Res. 192, 116852 https://doi.org/10.1016/J.WATRES.2021.116852.
Mukherjee, S., Jemielita, M., Stergioula, V., Tikhonov, M., Bassler, B.L., 2019. Photosensing and quorum sensing are integrated to control *Pseudomonas aeruginosa* collective behaviors. PLoS Biol. 17 https://doi.org/10.1371/journal.pbio.3000579.
Nalbone, L., Panebianco, A., Giarratana, F., Russell, M., 2021. Nile Red staining for detecting microplastics in biota: preliminary evidence. Mar. Pollut. Bull. 172, 112888 https://doi.org/10.1016/j.marpolbul.2021.112888.
OECD, 2022. OECD's work on co-operating in the investigation of high production volume chemicals - chemical detailed results [WWW Document]. URL. https://hpvchemicals.oecd.org/UI/SIDS_Details.aspx?key=c3c7c02a-dca0-48da-9eb9-9e36b88652be&idx=0. accessed 8.22.22.

Oh, E., Kim, J.-C., Jeon, B., 2016. Stimulation of biofilm formation by oxidative stress in *Campylobacter jejuni* under aerobic conditions. Virulence 7. https://doi.org/10.1080/21505594.2016.1197471.

Pabortsava, K., Lampitt, R.S., 2020. High concentrations of plastic hidden beneath the surface of the Atlantic Ocean. Nat. Commun. 11 https://doi.org/10.1038/s41467-020-17932-9.

Peng, X., Zhu, Z., Xiong, S., Fan, Y., Chen, G., Tang, C., 2020. Tissue distribution, growth dilution, and species-specific bioaccumulation of organic ultraviolet absorbents in wildlife freshwater fish in the pearl river catchment, China. Environ. Toxicol. Chem. 39, 343–351. https://doi.org/10.1002/etc.4616.

Pham, D.N., Clark, L., Li, M., 2021. Microplastics as hubs enriching antibiotic-resistant bacteria and pathogens in municipal activated sludge. J. Hazard. Mater. Lett. 2, 100014 https://doi.org/10.1016/J.HAZL.2021.100014.

Polychem-USA, 2021. Low density polyethylene (LDPE) manufacturing process [WWW Document]. URL. https://polychem-usa.com/low-density-polyethylene-manufacturing/. accessed 8.9.22.

Preda, V.G., Săndulescu, O., 2019. Communication is the key: biofilms, quorum sensing, formation and prevention. Discoveries 7. https://doi.org/10.15190/d.2019.13 e10.

Molecular Probes Inc., 2004. LIVE/DEAD® BacLight TM bacterial viability kits. Prod. Inf. 1–5.

Reimann, R., Zeng, B., Jakopec, M., Burdukiewicz, M., Petrick, I., Schierack, P., Rödiger, S., 2020. Classification of dead and living microalgae *Chlorella vulgaris* by bioimage informatics and machine learning. Algal Res. 48 https://doi.org/10.1016/J.ALGAL.2020.101908.

Ridler, T.W., Calvard, S., 1978. Picture thresholding using an interactive selection method. IEEE Trans. Syst. Man Cybern 630–632 smc-8.

Riga, E.K., Vöhringer, M., Widyaya, V.T., Lienkamp, K., 2017. Polymer-based surfaces designed to reduce biofilm formation: from antimicrobial polymers to strategies for long-term applications. Macromol. Rapid Commun. 38 https://doi.org/10.1002/MARC.201700216.

Scales, B.S., Cable, R.N., Duhaime, M.B., Gerdts, G., Fischer, F., Fischer, D., Mothes, S., Hintzki, L., Moldaenke, L., Ruwe, M., Kalinowski, J., Kreikemeyer, B., Pedrotti, M.L., Gorsky, G., Elineau, A., Labrenz, M., Oberbeckmann, S., 2021. Cross-hemisphere study reveals geographically ubiquitous , unexplored biosphere. Am. Soc. Microbiol. 6, 1–17.

Schieber, M., Chandel, N.S., 2014. ROS Function in Redox Signaling and Oxidative Stress. https://doi.org/10.1016/j.cub.2014.03.034.

Schlundt, C., Mark Welch, J.L., Knochel, A.M., Zettler, E.R., Amaral-Zettler, L.A., 2020. Spatial structure in the "Plastisphere": molecular resources for imaging microscopic communities on plastic marine debris. Mol. Ecol. Resour. 20, 620–634. https://doi.org/10.1111/1755-0998.13119.

Semcesen, P.O., Wells, M.G., 2021. Biofilm growth on buoyant microplastics leads to changes in settling rates: implications for microplastic retention in the Great Lakes. Mar. Pollut. Bull. 170 https://doi.org/10.1016/J.MARPOLBUL.2021.112573.

Shi, J., Wu, D., Su, Y., Xie, B., 2021. Selective enrichment of antibiotic resistance genes and pathogens on polystyrene microplastics in landfill leachate. Sci. Total Environ. 765, 142775 https://doi.org/10.1016/J.SCITOTENV.2020.142775.

Siedenbiedel, F., Tiller, J.C., 2012. Antimicrobial polymers in solution and on surfaces: overview and functional principles, 2012 Polymer 4, 46–71. https://doi.org/10.3390/POLYM4010046, 4, 46–71.

Sigma-Aldrich, 2021. Calcofluor White Stain suitable for microbiology [WWW Document]. URL. https://www.sigmaaldrich.com/MY/en/product/sial/18909. accessed 8.14.22.

Sjollema, S.B., Redondo-Hasselerharm, P., Leslie, H.A., Kraak, M.H.S., Vethaak, A.D., 2016. Do plastic particles affect microalgal photosynthesis and growth? Aquat. Toxicol. 170, 259–261. https://doi.org/10.1016/J.AQUATOX.2015.12.002.

Sullivan, T., 2019. Cell shape and surface colonisation in the diatom genus cocconeis-an opportunity to explore bio-inspired shape packing? Biomimetics 4. https://doi.org/10.3390/biomimetics4020029.

Taheri-Araghi, S., Guerbidjian, O., 2020. A layer of dead cells at the periphery protects biofilms from antimicrobial peptides. Biophys. J. 118, 382a. https://doi.org/10.1016/j.bpj.2019.11.2180.

Tanaka, K., Takada, H., Ikenaka, Y., Nakayama, S.M.M., Ishizuka, M., 2020. Occurrence and concentrations of chemical additives in plastic fragments on a beach on the island of Kauai. Hawaii. Mar. Pollut. Bull. 150, 110732 https://doi.org/10.1016/j.marpolbul.2019.110732.

Tarafdar, A., Sarkar, T.K., Chakraborty, S., Sinha, A., Masto, R.E., 2018. Biofilm development of *Bacillus thuringiensis* on MWCNT buckypaper: adsorption-synergic biodegradation of phenanthrene. Ecotoxicol. Environ. Saf. 157, 327–334. https://doi.org/10.1016/j.ecoenv.2018.03.090.

Tarafdar, A., Lee, J.U., Jeong, J.E., Lee, H., Jung, Y., Oh, H. Bin, Woo, H.Y., Kwon, J.H., 2021. Biofilm development of *Bacillus siamensis* ATKU1 on pristine short chain low-density polyethylene: a case study on microbe-microplastics interaction. J. Hazard Mater. 409, 124516 https://doi.org/10.1016/j.jhazmat.2020.124516.

Tarafdar, A., Choi, S.-H., Kwon, J.-H., 2022. Differential staining lowers the false positive detection in a novel volumetric measurement technique of microplastics. J. Hazard Mater. 432, 128755 https://doi.org/10.1016/j.jhazmat.2022.128755.

Tsering, T., Sillanpää, M., Viitala, M., Reinikainen, S.-P., 2022. Variation of microplastics in the shore sediment of high-altitude lakes of the Indian Himalaya using different pretreatment methods. Sci. Total Environ., 157870 https://doi.org/10.1016/J.SCITOTENV.2022.157870.

Tu, C., Chen, T., Zhou, Q., Liu, Y., Wei, J., Waniek, J.J., Luo, Y., 2020. Biofilm formation and its influences on the properties of microplastics as affected by exposure time and depth in the seawater. Sci. Total Environ. 734 https://doi.org/10.1016/j.scitotenv.2020.139237.

van der Kooij, D., Veenendaal, H.R., Baars-Lorist, C., van der Klift, D.W., Drost, Y.C., 1995. Biofilm formation on surfaces of glass and Teflon exposed to treated water. Water Res. 29, 1655–1662. https://doi.org/10.1016/0043-1354(94)00333-3.

Villa, F., Remelli, W., Forlani, F., Gambino, M., Landini, P., Cappitelli, F., 2012. Effects of chronic sub-lethal oxidative stress on biofilm formation by *Azotobacter vinelandii*. Biofouling 28, 823–833. https://doi.org/10.1080/08927014.2012.715285.

Wang, Z., Gong, X., Xie, J., Xu, Z., Liu, G., Zhang, G., 2019. Investigation of formation of bacterial biofilm upon dead siblings. Langmuir 35, 7405–7413. https://doi.org/10.1021/acs.langmuir.8b01962.

Wang, Jiaping, Li, G., Yin, H., An, T., 2020a. Bacterial response mechanism during biofilm growth on different metal material substrates: EPS characteristics, oxidative stress and molecular regulatory network analysis. Environ. Res. 185 https://doi.org/10.1016/J.ENVRES.2020.109451.

Wang, Jie, Qin, X., Guo, J., Jia, W., Wang, Q., Zhang, M., Huang, Y., 2020b. Evidence of selective enrichment of bacterial assemblages and antibiotic resistant genes by microplastics in urban rivers. Water Res. 183, 116113 https://doi.org/10.1016/J.WATRES.2020.116113.

Wang, H., Yu, P., Schwarz, C., Zhang, B., Huo, L., Shi, B., Alvarez, P.J.J., 2022a. Phthalate esters released from plastics promote biofilm formation and chlorine resistance. Environ. Sci. Technol. 56, 1081–1090. https://doi.org/10.1021/acs.est.1c04857.

Wang, W., Lee, I.S., Oh, J.E., 2022b. Specific-accumulation and trophic transfer of UV filters and stabilizers in marine food web. Sci. Total Environ. 825, 154079 https://doi.org/10.1016/J.SCITOTENV.2022.154079.

Wick, A., Jacobs, B., Kunkel, U., Heininger, P., Ternes, T.A., 2016. Benzotriazole UV stabilizers in sediments, suspended particulate matter and fish of German rivers: new insights into occurrence, time trends and persistency. Environ. Pollut. 212, 401–412. https://doi.org/10.1016/j.envpol.2016.01.024.

Wright, R.J., Erni-Cassola, G., Zadjelovic, V., Latva, M., Christie-Oleza, J.A., 2020. Marine plastic debris: a new surface for microbial colonization. Environ. Sci. Technol. 54, 11657–11672. https://doi.org/10.1021/acs.est.0c02305.

Wright, R.J., Bosch, R., Langille, M.G.I., Gibson, M.I., Christie-Oleza, J.A., 2021. A multi-OMIC characterisation of biodegradation and microbial community succession within the PET plastisphere. Microbiome 9, 1–22. https://doi.org/10.1186/S40168-021-01054-5/FIGURES/4.

Wu, Y., Guo, P., Zhang, X., Zhang, Y., Xie, S., Deng, J., 2019. Effect of microplastics exposure on the photosynthesis system of freshwater algae. J. Hazard Mater. 374, 219–227. https://doi.org/10.1016/J.JHAZMAT.2019.04.039.

Xiong, X., Tappenbeck, T.H., Wu, C., Elser, J.J., 2022. Microplastics in Flathead Lake, a large oligotrophic mountain lake in the USA. Environ. Pollut. 306, 119445 https://doi.org/10.1016/J.ENVPOL.2022.119445.

Yang, G., Gong, M., Mai, L., Zhuang, L., Zeng, E.Y., 2021. Diversity and structure of microbial biofilms on microplastics in riverine waters of the Pearl River Delta, China. Chemosphere 272, 129870. https://doi.org/10.1016/j.chemosphere.2021.129870.

Ye, G., Zhang, X., Yan, C., Lin, Y., Huang, Q., 2021. Polystyrene microplastics induce microbial dysbiosis and dysfunction in surrounding seawater. Environ. Int. 156, 106724 https://doi.org/10.1016/j.envint.2021.106724.

Zhang, Z., Ren, N., Li, Y.F., Kunisue, T., Gao, D., Kannan, K., 2011. Determination of benzotriazole and benzophenone UV filters in sediment and sewage sludge. Environ. Sci. Technol. 45, 3909–3916. https://doi.org/10.1021/es2004057.

Zhao, S., Zettler, E.R., Amaral-Zettler, L.A., Mincer, T.J., 2021. Microbial carrying capacity and carbon biomass of plastic marine debris. ISME J. 15, 67–77. https://doi.org/10.1038/s41396-020-00756-2.